RSPH3 Mutations Cause Primary Ciliary Dyskinesia with Central-Complex Defects and a Near Absence of Radial Spokes

Ludovic Jeanson,[1,13] Bruno Copin,[2,13] Jean-François Papon,[3,4] Florence Dastot-Le Moal,[2] Philippe Duquesnoy,[1] Guy Montantin,[2] Jacques Cadranel,[5,6] Harriet Corvol,[7,8] André Coste,[3,9] Julie Désir,[10] Anissa Souayah,[11] Esther Kott,[1] Nathalie Collot,[2] Sylvie Tissier,[2] Bruno Louis,[3] Aline Tamalet,[7] Jacques de Blic,[12] Annick Clement,[1,7] Estelle Escudier,[1,2] Serge Amselem,[1,2,*] and Marie Legendre[1,2]

Primary ciliary dyskinesia (PCD) is a rare autosomal-recessive condition resulting from structural and/or functional defects of the axoneme in motile cilia and sperm flagella. The great majority of mutations identified so far involve genes whose defects result in dynein-arm anomalies. By contrast, PCD due to CC/RS defects (those in the central complex [CC] and radial spokes [RSs]), which might be difficult to diagnose, remains mostly unexplained. We identified non-ambiguous *RSPH3* mutations in 5 of 48 independent families affected by CC/RS defects. *RSPH3*, whose ortholog in the flagellated alga *Chlamydomonas reinhardtii* encodes a RS-stalk protein, is mainly expressed in respiratory and testicular cells. Its protein product, which localizes within the cilia of respiratory epithelial cells, was undetectable in airway cells from an individual with *RSPH3* mutations and in whom RSPH23 (a RS-neck protein) and RSPH1 and RSPH4A (RS-head proteins) were found to be still present within cilia. In the case of *RSPH3* mutations, high-speed-videomicroscopy analyses revealed the coexistence of immotile cilia and motile cilia with movements of reduced amplitude. A striking feature of the ultrastructural phenotype associated with *RSPH3* mutations is the near absence of detectable RSs in all cilia in combination with a variable proportion of cilia with CC defects. Overall, this study shows that *RSPH3* mutations contribute to disease in more than 10% of PCD-affected individuals with CC/RS defects, thereby allowing an accurate diagnosis to be made in such cases. It also unveils the key role of *RSPH3* in the proper building of RSs and the CC in humans.

Primary ciliary dyskinesia (PCD [MIM: 244400]) comprises a heterogeneous group of autosomal-recessive disorders affecting one in 15,000–30,000 individuals, although it has a higher incidence in both individuals born to consanguineous unions and some isolated populations.[1] This disease, which results from structural and/or functional defects of cilia, leads to impaired mucociliary transport, which is responsible for neonatal respiratory distress and chronic respiratory infections of the upper and lower airways (i.e., sinusitis and bronchiectasis). Male and female subfertility occurs as a result of defective sperm flagella and oviduct cilia, respectively.[2]

Eukaryotic cilia and flagella are evolutionarily conserved organelles that are composed of hundreds of conserved proteins for building the axoneme, a highly ordered microtubule-based structure[3] consisting of nine peripheral microtubule doublets (A and B) with or without a central pair of microtubules (9+2 or 9+0 pattern, respectively). The 9+0 cilia are immotile, except those present in the embryonic node, a structure that governs left-right asymmetry.[4] The 9+2 cilia, which are motile, contain inner dynein arms (IDAs), outer dynein arms (ODAs), and radial spokes (RSs). ODAs and IDAs are ATPase complexes anchored on peripheral doublets, where they constitute the motor generating the ciliary and flagellar movements.[5] RSs are T-shaped structures that are anchored on the A-tubule of each outer doublet through the spoke stalk (vertical bar of the "T").[6] The spoke heads (horizontal bar of the "T") project inward, toward the central complex (CC; i.e., two central microtubules surrounded by a central sheath), and transiently interact with the central-pair projections.[7] These RS interactions are believed to transmit a mechanochemical signal to outer microtubule doublets and locally control dynein-driven microtubule sliding.[8,9] In the flagellated alga *Chlamydomonas reinhardtii*, the RSs are composed of at least 23 proteins.[6] However, a recent study performed on respiratory cilia by means of cryo-electron

[1]INSERM UMR S933, Université Pierre et Marie Curie (Paris 6), Sorbonne Universités, Paris 75012, France; [2]Service de Génétique et Embryologie Médicales, Hôpital Armand Trousseau, Assistance Publique – Hôpitaux de Paris, Paris 75012, France; [3]INSERM UMR S955, Equipe 13, Université Paris-Est Créteil, Créteil 94000, France; [4]Service d'Oto-Rhino-Laryngologie et de Chirurgie Cervico-Maxillo-Faciale, Hôpital Bicêtre, Assistance Publique – Hôpitaux de Paris, Le Kremlin-Bicêtre 94275, France; [5]Service de Pneumologie-Centre Expert Maladies Pulmonaires Rares, Hôpital Tenon, Assistance Publique – Hôpitaux de Paris, Paris 75020, France; [6]Université Pierre et Marie Curie (Paris 6), Sorbonne Universités, Paris 75020, France; [7]Service de Pneumologie Pédiatrique, Hôpital Armand Trousseau, Assistance Publique – Hôpitaux de Paris and Centre National de Référence des Maladies Respiratoires Rares, Paris 75012, France; [8]INSERM UMR S938, Université Pierre et Marie Curie (Paris 6), Sorbonne Universités, Paris 75012, France; [9]Service d'Oto-Rhino-Laryngologie et de Chirurgie Cervico-Faciale, Hôpital Intercommunal et Groupe Hospitalier Henri Mondor-Albert Chenevier, Assistance Publique – Hôpitaux de Paris, Créteil 94000, France; [10]Département de Génétique Médicale, Université Libre de Bruxelles and Hôpital Erasme, Brussels 1020, Belgium; [11]Service d'Oto-Rhino-Laryngologie, Hôpital Universitaire des Enfants Reine Fabiola, Brussels 1020, Belgium; [12]Service de Pneumologie et Allergologie Pédiatriques, Groupe Hospitalier Necker-Enfants Malades, Assistance Publique – Hôpitaux de Paris and Université Paris Descartes, Paris 75015, France
[13]These authors contributed equally to this work
*Correspondence: serge.amselem@inserm.fr
http://dx.doi.org/10.1016/j.ajhg.2015.05.004.

Table 1. Phenotypic Features of Individuals with Identified *RSPH3* Mutations

Individual	Family (Origin)	Known Consanguinity	Gender (Age)	Airway Disease	Fertility	NO[a]	CBF[b] (Hz)	Allele 1	Allele 2
PCD1183	DC628 (North African)	yes	male (52 years)	NRD, bronchiectasis, COPD, rhinosinusitis, otitis	infertility	NP	6	c.616C>T (p.Gln206*)	c.616C>T (p.Gln206*)
PCD9	DC156 (North African)	yes	male (12 years)	bronchiectasis, pneumopathies, rhinosinusitis, otitis	NR	low[c]	10	c.631−2A>G	c.631−2A>G
PCD331	DC141 (North African)	yes	male (15 years)	bronchiectasis, pneumopathies, rhinosinusitis, otitis	NR	low[c]	0	c.616C>T (p.Gln206*)	c.616C>T (p.Gln206*)
PCD751	DC466 (Central African)	no	female (33 years)	NRD, bronchiectasis, rhinosinusitis, otitis	NA	NP	0	c.1192C>T (p.Arg398*)	c.1320_1323delTGAA (p.Asn440Lysfs*19)
PCD833	DC100 (European)	no	female (45 years)	NRD, bronchiectasis, rhinosinusitis, otitis	infertility	0 nl/mn	10	c.631−2A>G	c.1105C>T (p.Arg369*)

Abbreviations are as follows: NO, nitric oxide; TEM, transmission electron microscopy; NRD, neonatal respiratory distress; COPD, chronic obstructive pulmonary disease; NR, not relevant; NA, not available; NP, not performed; CBF, ciliary beat frequency.
[a]Nasal NO was measured during apnea with the use of a chemoluminescence NO analyzer (NIOX Flex, Aerocrine; Endono 8000, Seres). The mean value of the plateau was recorded. NO values above 100 nl/min were considered normal.
[b]CBF was measured by optical microscopy analysis as described by Tamalet et al.[45]
[c]Value not available.

tomography has revealed that RSs are structurally different in humans.[10]

Several genes that play a key role in the proper building of motile cilia are known to be involved in the pathogenesis of PCD. The great majority of mutations identified so far involve genes whose defects result in dynein-arm anomalies.[11–33] Other gene defects have been identified in some individuals with PCD and no detectable structural anomaly of the axoneme.[34–36] In approximately 50% of all these PCD cases, the disease can be associated with total situs inversus (Kartagener syndrome [MIM: 244400]) or more severe laterality defects, such as cardiac malformations.[37] Notably, individuals with PCD due to CC abnormalities have no laterality defects, a feature explained by the physiologic absence of CC in the nodal motile cilia. Very few genes have been found to be involved in this PCD phenotype: three (*RSPH4A*[38,39] [MIM: 612647], *RSPH9*[38,40] [MIM: 612648], and *RSPH1*[41] [MIM: 609314]) encode proteins constitutive of the spoke head, and one (*HYDIN*[42] [MIM: 610812]) has been implicated in a subgroup of PCD characterized by central-sheath defects. Overall, in spite of these significant results, the disease is explained in less than half of affected individuals from our PCD cohort, in which the CC-defect phenotype represents almost 15% of the cases.

The aim of the present study was to identify genes involved in PCD due to CC defects by using a combination of homozygosity mapping and whole-exome sequencing (WES) followed by Sanger sequencing of a candidate gene in a large cohort of individuals with CC defects. The current study was approved by the Ile-de-France ethics committee (approval no. CPP07729), and written consent was obtained from all individuals and/or their parents. Forty-eight unrelated families (including 62 affected individuals) of our PCD cohort are affected by CC defects; none of them are affected by laterality defects. In all of them, the axonemal defect was assessed by transmission electronic microscopy (TEM). The ultrastructural phenotype of individuals with PCD due to CC defects is characterized by a variable proportion of cilia displaying an absence of one or two microtubules of the central pair (9+1 or 9+0 pattern, respectively) and is sometimes associated with a disorganized configuration and/or a transposition of one peripheral doublet (8+1 pattern);[43–45] disorganized cilia with a 9+2 pattern are also observed with variable frequency.[43–45] By screening the genes already involved in PCD due to CC defects, we identified biallelic mutations in 21 of the 48 independent families: *RSPH4A* mutations in seven families, *RSPH9* mutations in four families, and *RSPH1* mutations in ten families.[41] One individual (PCD1183 from family DC628) of the 27 remaining unrelated families (32 affected individuals) exhibited marked ultrastructural anomalies with CC defects (37% of cilia) and almost no detectable RSs in all cilia (RSs only very rarely present in some cilia with a 9+2 pattern), as well as a low ciliary beat frequency (CBF; 6 Hz), as assessed by optic microscopy on airway brushing.[45] This individual, who was born to a consanguineous union, was selected for homozygosity mapping and WES analysis. He displayed neonatal respiratory distress, chronic obstructive pulmonary disease, bronchiectasis, rhino-sinusitis, otitis, and infertility. Detailed phenotypic features are presented in Table 1 and Figure 1. His genomic DNA was first genotyped with the HumanCytoSNP-12 chip from Illumina, and the data were analyzed with GenomeStudio and CNVPartition v.3.1.6 (Illumina). This analysis led to the identification of 13 large regions of homozygosity, which contain a total of 1,440 genes (Figure S1 and Table S1).

Nonsense, missense, and frameshift variants were identified by WES, performed by IntegraGen with the Agilent

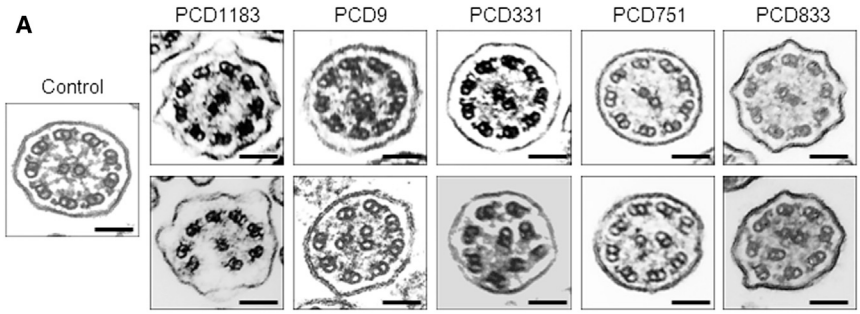

B

Ciliary Defects Identified by TEM in Individuals with *RSPH3* Mutations

Individuals	9+2 (%)	9+2 (%) disorganized	9+0 (%) regular	9+0 (%) disorganized	8+1 (%) transposition	Additional minor defects
PCD1183	63.0	7.2	16.0	7.2	6.6	Supernumerary microtubules
PCD9	65.4	30.6	0.0	2.0	2.0	Partial lack of IDAs and ODAs
PCD331	32.0	26.0	10.0	22.0	10.0	Partial lack of IDAs
PCD751	18.3	32.3	5.7	15.0	28.7	Partial lack of ODAs
PCD833	56.3	14.0	6.3	3.0	20.4	Supernumerary microtubules

Figure 1. CC/RS Defects in Respiratory Cilia of Individuals with *RSPH3* Mutations
(A) The electron micrographs of cross-sections of cilia from a control individual and five individuals with identified *RSPH3* mutations are shown. For each affected individual, two sections are shown: one with a well-organized configuration (9+2) showing the presence of the CC but with a near absence of RSs (top) and another with an abnormal axonemal configuration (9+2 disorganized or 8+1 transposition) and no detectable RSs (bottom). Black scale bars represent 0.1 μm.
(B) Distribution of the different ciliary defects (expressed as a percentage of abnormal cilia) identified by TEM in individuals with *RSPH3* mutations. Reference values are those from the TEM study performed by Rossman et al. on 55 control (non-atopic non-smoker healthy) individuals: the proportion of cilia with a normal ultrastructure is 95.2% ± 3.5%, whereas that of cilia with a missing CC is 0.4% ± 0.8%.[46] Abbreviations are as follows: IDA, inner dynein arms; ODA, outer dynein arms.

SureSelect All Exon V5+UTRs 70-Mb Capture Kit on a HiSeq 2000 (quality criteria are provided in Table S2). Overall, 224,730 variations were identified in individual PCD1183. The identified variants were filtered against those in several sequence-variant databases (i.e., dbSNP 132, 1000 Genomes, and the NHLBI Exome Sequencing Project Exome Variant Server). Following an autosomal-recessive model for PCD, we considered further the gene variants that are located in homozygous regions and that are not described in these databases or are described with frequencies compatible with the incidence of PCD (the maximal theoretical frequency of a PCD allele is about 0.008). Among those 1,846 variations, 1,834 were located in non-coding regions, and among the 12 located in coding regions, six corresponded to missense variations, five were synonymous, and only one was a homozygous nonsense variant. We then focused our attention on the sequence variants located in genes whose function and/or expression profiles (in the testes, trachea, and lungs) were compatible with PCD. Among those candidate genes, only one (*RSPH3* [MIM: 615876]) had a clear ciliary function, and it was the gene that contained the homozygous nonsense variant. This sequence variation (c.616C>T), found in a large region of homozygosity in chromosomal region 6q25.3 (10.3 Mb), leads to a stop codon at position 206 (p.Gln206*) in the second exon of *RSPH3*. This variation has not been described in genomic-variant databases such as dbSNP, 1000 Genomes, the Exome Variant Server, or the Exome Aggregation Consortium (ExAC) Browser. *RSPH3* contains eight exons; the only validated transcript (GenBank: NM_031924.4) encodes a 560-residue protein with, as predicted by SMART, a radial spoke 3 domain (RS3D) containing an RIIa-domain-binding amphipathic helix (AH_R)[47] and two coiled-coil domains (Figure 2). RSPH3 is the homolog of *Chlamydomonas reinhardtii* RSP3, which contains six functional domains that are well conserved in human RSPH3 (Figure 2). Each of these domains interacts with specific protein partners. The axoneme targeting domain has been shown to bind to the axoneme, probably in an indirect manner;[48] the AH_R domain has been shown to directly interact with protein kinase A[47,49] and RSP11 (the ortholog of human ROPN1L, also named RSPH11).[49] The Dpy-30-domain-binding amphipathic helix (AH_D) has been shown to directly interact with RSP2 (the ortholog of human DYDC1) and RSP23 (the ortholog of human NME5, also named RSPH23),[50] whereas the three TQT-like domains have been found to interact directly with a LC8 (the ortholog of human DYNLL1) dimer.[51] As proposed by Sivadas et al.,[50] RSP3, which is a RS-stalk protein, forms a dimer that constitutes the core of each RS and has two sites for anchoring RSP7 and RSP11 at the A-tubule of the outer-doublet side and RSP2 and RSP23 (two RS-neck proteins) at the central-pair side. In individual PCD1183, p.Gln206* (the consequence of the c.616C>T transition) is therefore expected to be highly deleterious at the protein level: mutated *RSPH3* transcripts would generate a severely

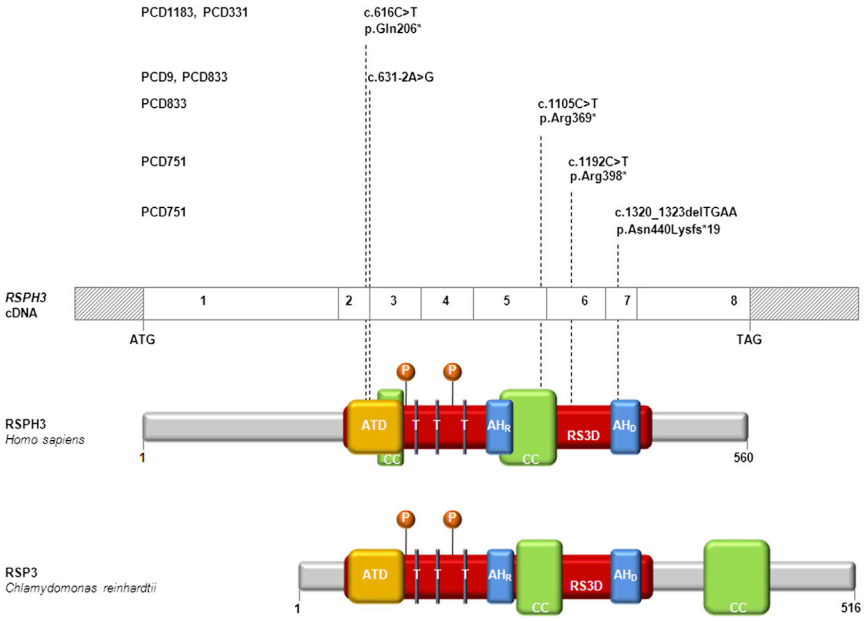

Figure 2. *RSPH3* Mutations and Their Impact at the Protein Level in Individuals with PCD

Exonic organization of the human *RSPH3* cDNA containing the mutations for the five families described in this study (top). Domain-organization models of the corresponding protein (middle) and of the *Chlamydomonas reinhardtii* orthologous RSP3 (bottom) are also shown. The eight exons are indicated by empty or hashed boxes, which depict translated or untranslated sequences, respectively. According to the predictions by SMART and literature, RSPH3 is composed of a radial spoke 3 domain (RS3D, in red) containing an axoneme targeting domain (ATD, in yellow), a RIIa-domain-binding amphipathic helix (AH_R, in blue), a Dpy-30-domain-binding amphipathic helix (AH_D, in blue), three TQT-like LC8-binding motifs (T, in purple), two coil-coiled domains (CC, in green), and two phosphorylated threonines (P, orange circle).

truncated protein lacking the six functional domains. Alternatively, this sequence variant might trigger the nonsense-mediated mRNA decay (NMD) pathway and lead to the absence of protein production. Sanger sequencing was performed to validate the c.616C>T mutation found in PCD1183 (Figure S2 and Table S3). Parental DNA samples were not available; however, as deduced from the homozygosity mapping data (Figure S1), the c.616C>T transition is indeed present in the homozygous state in PCD1183.

The remaining 26 independent families (30 affected individuals) affected by PCD due to CC defects and with no mutations in *RSPH1*, *RSPH4A*, or *RSPH9* were subsequently screened for *RSPH3* mutations. Overall, four individuals (PCD9, PCD331, PCD751, and PCD833 from families DC156, DC141, DC466, and DC100, respectively) were found to carry *RSPH3* mutations (Table 1, Figure 2, and Figure S2). Notably, all the individuals with CC defects and identified *RSPH3* mutations display a near absence of RSs in all examined cilia (RSs only very rarely present in some cilia with a 9+2 pattern). The disease phenotype of these individuals is detailed in Table 1 and Figure 1. PCD9 carries a transition (c.631−2A>G) that affects the splice acceptor site of intron 2 (Table 1 and Figure 2). This mutation, which destroys the invariant AG sequence of the consensus site for mRNA processing,[52] is therefore deleterious. Both parents were found to be heterozygous for the mutation. This variation is reported in 1000 Genomes and the ExAC Browser (rs142800871) at very low frequencies (allele frequencies = 0.00092 and 0.000067, respectively; Table S4) and is not reported to be homozygous in 1,092 and 60,044 individuals, respectively. Given these allele frequencies, the expected frequency of the homozygous genotype should be extremely low (4.356×10^{-9} to 8.464×10^{-7}), in keeping with the fact that PCD is a rare disease. Individual PCD331 carries the same homozygous variation as PCD1183: c.616C>T, which leads to a premature stop codon at position 206 (p.Gln206*; Table 1 and Figure 2). As deduced from the homozygosity mapping data, this individual was born to a consanguineous union (Figure S3). Individuals PCD1183 and PCD331 share both a 6-Mb homozygous region that contains *RSPH3* and a common haplotype spanning 460 SNPs (Figure S4), thereby supporting a founder effect. PCD751 carries two heterozygous *RSPH3* variants: a transition (c.1192C>T) introducing a premature stop codon (p.Arg398*) and a 4-nt deletion (c.1320_1323delTGAA) that would introduce a frameshift leading to a stop codon at position 459 (p.Asn440Lysfs*19). These two sequence variants with expected deleterious consequences at the protein level (i.e., premature stop codon leading either to a truncated protein lacking the AH_D domain or to the absence of protein production through activation of the NMD pathway) are in *trans*, as shown after the sequencing of cloned PCR products encompassing the two mutation sites (with pCR2.1-TOPO plasmids and chemocompetent *E. coli* from Invitrogen; data not shown). PCD833 also carries two heterozygous *RSPH3* variants. Although compound heterozygosity could not be demonstrated in this individual, it is very likely that these two unambiguous mutations are in *trans*. The first variation is the c.631−2A>G splice-site mutation, which was already found in PCD9. The second variation (c.1105C>T) would lead to a stop codon at position 369 (p.Arg369*; Table 1 and Figure 2). This nonsense mutation, which has not been described in databases of genomic variants, would lead either to a truncated RSPH3 lacking both the AH_D domain and a part of a coiled-coil domain or to the absence of protein production (Figure 2).

To gain further insight into the role of RSPH3, we first determined its tissue expression by qRT-PCR. The analysis revealed that *RSPH3* is readily expressed in tissues with

motile cilia or flagella, such as trachea, lung, and testis tissues and tissues obtained by airway brushings (Figure S5). This expression pattern is typical of genes already implicated in PCD. The access to ciliated cells obtained by airway brushing in one of the individuals with biallelic *RSPH3* mutations (individual PCD9) allowed us to study by high-speed videomicroscopy (according to the protocol described by Papon et al.[53]) the ciliary motion in this individual compared to that in healthy control individuals. In brief, beating ciliated edges were recorded with a high-speed digital camera (PixeLINK A741) with a 100× objective at a rate of 355 frames per second. The percentage of beating cilia was determined, and ten cilia able to be followed during a complete beating cycle were then selected in distinct areas. We collected several measurements made on cilia in order to determine the following objective parameters: the CBF, the beating angle, and the distance traveled by the tip of the cilium per second. Different populations of cilia were identified in individual PCD9 (Table S5): some cilia were immotile whereas others displayed a low CBF with an abnormal beating pattern characterized by movements of reduced amplitude (i.e., diminished beating angle and reduced distance traveled by the cilia's tips). One representative movie of a control individual and one representative movie of individual PCD9 are presented as supplemental data (Movies S1 and S2, respectively).

We subsequently determined RSPH3 subcellular localization in ciliated cells by means of immunofluorescence microscopy with an anti-RSPH3 antibody. This was performed in human ciliated cells collected by nasal brushing from a healthy control individual and from individual PCD9, who has biallelic *RSPH3* mutations. Airway cells from the healthy control individual showed RSPH3 labeling, together with acetylated α-tubulin labeling, within the cilia (Figures 3A–3C); by contrast, RSPH3 was not detected in cilia from individual PCD9 (Figures 3A′–3C′). This result, which confirms the specificity of the labeling obtained with the RSPH3 antibody used in this experiment, is consistent with the loss of function expected from the homozygous mutation identified in individual PCD9.

To test whether mutations in *RSPH3*, a gene whose ortholog in *Chlamydomonas reinhardtii* encodes a RS-stalk protein,[50] might affect the subcellular localization of other RS proteins, we first determined the subcellular localization of RSPH23 (a RS-neck protein) and RSPH1 and RSPH4A (two RS-head proteins) in ciliated cells from a healthy control individual (Figures 3D–3L) and from individual PCD9 (Figures 3D′–3L′). In airway cells from the control individual, we observed that ciliary labeling of those three proteins was similar to that obtained with the anti-RSPH3 antibody. Notably, in the individual with *RSPH3* mutations, RSPH23, RSPH1, and RSPH4A were still detected within the cilia (Figures 3D′–3L′). This observation is reminiscent of the observation made in a case of PCD due to a premature stop mutation in *RSPH9* (a RS-head protein); in this case, RSPH1 and RSPH4A were also detected within the cilia.[54] We then tested whether mutations in *RSPH3* might affect the subcellular localization of RSPH11, a protein located at the base of the RS stalk and whose ortholog (RSP11) interacts directly with RSP3 in *Chlamydomonas reinhardtii*.[49] The RSPH11 labeling, which was easily detectable within cilia from a control individual (Figures 3M–3O), was not detectable in the airway cells of individual PCD9 (Figures 3M′–3O′), in keeping with the data obtained in the *Chlamydomonas reinhardtii* mutant *pf14*, which carries a premature stop codon in RSP3 (p.Trp63*).[55] Finally, we also tested whether mutations in *RSPH3* might affect the subcellular localization of DNALI1, an IDA component. We observed ciliary labeling in airway cells from both a control individual (Figures 3P–3R) and individual PCD9 (Figures 3P′–3R′), a result that is consistent with the TEM images showing the presence of IDAs in cilia of individuals with *RSPH3* mutations (Figure 1A).

Notably, the phenotype of the flagella from *Chlamydomonas reinhardtii* mutant *pf14* is different from the phenotype of cilia from individuals with mutations in *RSPH3*. First, the *pf14* strain displays paralyzed flagella with a 9+2 microtubule configuration and a total absence of RSs,[48,55] whereas individuals with *RSPH3* mutations (and in whom 18.3%–65.4% of cilia have a 9+2 microtubule configuration) display additional microtubule configurations (i.e., regular 9+0 pattern, disorganized 9+0 pattern, and 8+1 pattern with transposition) and rarely present RSs. Similarly, the flagella of *Chlamydomonas reinhardtii* mutants *pf1* and *pf17* (each with a premature stop codon, in *RSP4* and *RSP9*, respectively) display a 9+2 microtubule configuration, whereas in humans, mutations in the corresponding homologs (*RSPH4A* and *RSPH9*, respectively) lead to cilia with various ultrastructural patterns (i.e., 9+2 pattern, regular 9+0 pattern, disorganized 9+0 pattern, and 8+1 pattern with transposition).[38,56] Second, individuals with mutations in *RSPH3* can have motile cilia, whereas, as mentioned, in the RSP3-deficient *Chlamydomonas reinhardtii* strain, the flagella are paralyzed. Such differences in ciliary and flagellar motility between humans and *Chlamydomonas* have also been reported for other PCD-associated genes (e.g., *RSPH4A* and *RSP4*[54,56] or *RSPH9* and *RSP9*[54,56]) in which loss-of-function mutations lead to motile cilia in humans and paralyzed flagella in *Chlamydomonas*. Third, the flagella of the *Chlamydomonas reinhardtii* mutant *pf14* lack RS-neck and RS-head proteins, whereas as shown in the current study, in the case of biallelic mutations in *RSPH3*, RSPH23 (RS-neck protein) and RSPH1 and RSPH4A (RS-head proteins) are still present within the cilia. Similarly, RSP1 and RSP4 (the orthologs of RSPH1 and RSPH4A, respectively) have been shown to be absent from the flagella of the *Chlamydomonas reinhardtii* mutant *pf17*, which carries a premature stop codon in *RSP9* (the ortholog of *RSPH9*),[57] whereas in an individual with a nonsense homozygous mutation (c.466C>T [p.Arg156*]) in *RSPH9*,[54] RSPH1 and RSPH4A have been

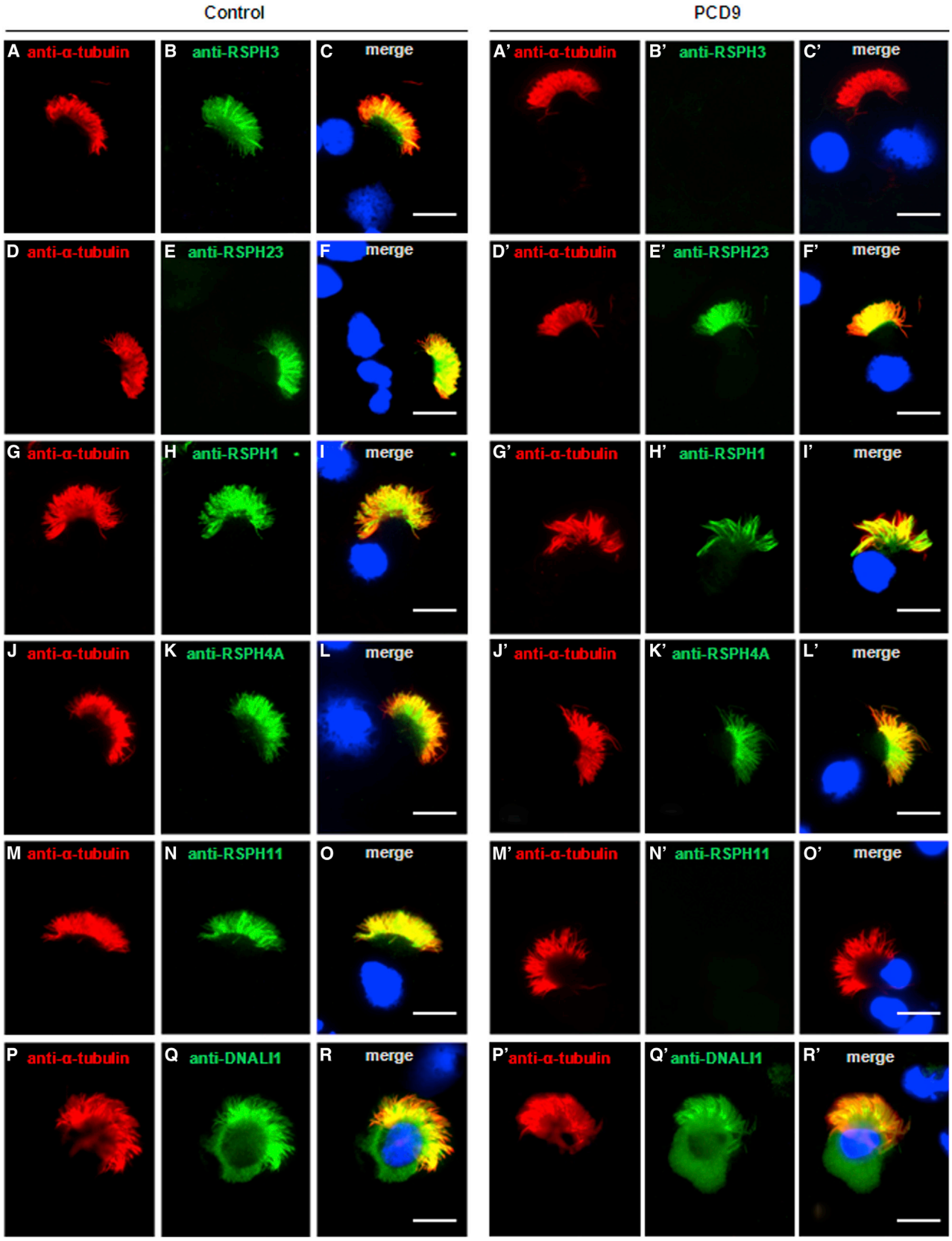

Figure 3. Localization of RSPH3 and Other Ciliary Proteins in Airway Epithelial Cells from a Healthy Individual and Individual PCD9
RSPH3 (green) localized within cilia (red) of the airway epithelial cells of a healthy control (A–C) and was absent from the cilia of individual PCD9 (A′–C′). RSPH23 (D–F and D′–F′), RSPH1 (G–I and G′–I′), and RSPH4A (J–L and J′–L′) (all in green) localized within cilia (red) of the airway epithelial cells of a healthy control individual and of individual PCD9. RSPH11 (green) localized within cilia (red) of

(legend continued on next page)

shown to be still present within the cilia. It is, however, important to note that the detection of RS proteins in *Chlamydomonas reinhardtii* was performed by means of proteomic analyses, whereas detection was performed in humans by means of immunofluorescence analyses. Overall, these observations, together with the fact that the human nodal cilia are motile in spite of the absence of RSs and the CC,[58] strongly suggest that the RSs are absolutely required for the motility of the *Chlamydomonas reinhardtii* flagella but not for the motility of all cilia in humans. In the case of *RSPH3* mutations, the presence of RSPH1, RSPH4A, and RSPH23 in cilia therefore supports the fact that RSPH3 is not required for the transport of these RS proteins into cilia and that the mechanisms underlying the assembly and transport of the RS components differ between humans and *Chlamydomonas*.

Whereas individuals with mutations in *RSPH1*, *RSPH4A*, or *RSPH9* exhibit CC defects, the ultrastructural phenotype associated with individuals with mutations in *RSPH3* is characterized by an additional feature corresponding to the near absence of RSs. Overall, these data raise the larger question of the respective role of these RSPH proteins in the proper building of RSs. It is well established that the axoneme is composed of 96-nm-long repeat units and that, in humans, each repeat contains three complete RSs (RS1, RS2, and RS3).[10] As shown by cryo-electron tomography, RS1 and RS2 are clearly separated from each other, whereas RS3, which is structurally different from RS1 and RS2, connects to the RS2 head.[10] In *Chlamydomonas reinhardtii*, the axonemal repeat is composed of two complete RSs (RS1 and RS2) and a reduced RS (RS3) lacking the spoke head and almost all the stalk, whereas RS3 is complete in human cilia.[10] As shown by cryo-electron tomography,[10] *RSPH1*-mutant PCD cilia display truncated RS1s and RS2s (with no head spoke), but intact RS3s, in keeping with the fact that RSs are readily detectable by conventional TEM in those individuals.[10,41] The *Chlamydomonas reinhardtii* mutant *pf14*, which has a nonsense mutation in *RSP3*, has no detectable RSs and lacks RS1 and RS2.[55] In light of all these data, it is therefore expected that in the case of *RSPH3* mutations, RS1 and RS2 could also be absent. Given the near absence of detectable RSs in *RSPH3*-mutant PCD cilia, it is tempting to speculate that the very few remaining RSs are of the RS3 type. It is, however, so far unknown whether RS3 contains RSPH3. Taken together, these data underline the fact that, in spite of the major interest in *Chlamydomonas reinhardtii* for understanding the pathophysiology of PCD, this flagellated alga does not represent a perfect model for human PCD.

In summary, our study shows that mutations in *RSPH3* lead to PCD with an abnormal axonemal configuration characterized by a near absence of RSs in all cilia, and a variable proportion of cilia with CC defects, thereby unveiling the key importance of RSPH3 in the proper building of RSs and the CC. It is often difficult to diagnose PCD in individuals with CC defects. Indeed, as mentioned above, individuals with PCD due to CC defects never display situs inversus. Second, as shown in individuals PCD1183, PCD9, and PCD833, ciliary beating can be observed in such individuals. In addition, individuals with PCD due to CC defects (and, as shown here, even individuals with the same genotype) display ultrastructural defects in variable proportions of their cilia[45,59] (i.e., 37% and 68% in PCD331 and PCD1183, respectively). This underlines the major interest of molecular analyses to confirm the diagnosis of PCD due to CC/RS defects. The contributions of *RSPH4A*, *RSPH9*, *RSPH1*, and *RSPH3* mutations to the PCD phenotype characterized by CC/RS defects in our national cohort of 48 unrelated families affected by this ultrastructural phenotype are the following: 14.6% (7/48), 8.3% (4/48), 20.8% (10/48), and 10.4% (5/48) of the cases, respectively. Mutations in these four genes therefore explain 53.1% of PCD cases due to CC/RS defects, which is a strong argument for the existence of an important genetic heterogeneity underlying this PCD phenotype.

Supplemental Data

Supplemental Data include five figures, five tables, and two movies and can be found with this article online at http://dx.doi.org/10.1016/j.ajhg.2015.05.004.

Acknowledgments

We are grateful to the affected persons and their families, whose cooperation made this study possible, and we thank all referring physicians. We thank Anne-Marie Vojtek and Catherine Faucon for their high-quality technical assistance for transmission-electronic-microscopy studies. This work was supported by grants from the Fondation pour la Recherche Médicale (DEQ20120323689), the Legs Poix from the Chancellerie des Universités, and the Milena Carvajal ProKartagener Foundation.

Received: March 9, 2015
Accepted: May 5, 2015
Published: June 11, 2015

the airway epithelial cells of a healthy control individual (M–O) but was absent from the cilia of individual PCD9 (M′–O′). DNALI1 (P–R and P′–R′) (in green) localized within cilia (red) of the airway epithelial cells of a healthy control individual and of individual PCD9. Airway epithelial cells were examined after labeling with rabbit polyclonal antibodies directed against RSPH3 (Novus Biological NBP1-84244, 1:100, 37°C, 1 hr), RSPH23 (Sigma HPA044555, 1:200, 37°C, 1 hr), RSPH1 (Sigma HPA017382, 1:200, 37°C, 1 hr), RSPH4A (Sigma HPA031196, 1:200, 37°C, 1 hr), RSPH11 (Sigma HPA039193, 1:200, 37°C, 1 hr), or DNALI1 (Abcam ab87075, 1:400, 37°C, 1 hr) and a secondary goat anti-rabbit Alexa Fluor 488 (green) antibody (Invitrogen A11034). For control individuals, we used an antibody directed against acetylated α-tubulin (mouse monoclonal [6-11B-1], Abcam ab24610, 1:700) to visualize microtubules, revealed by a secondary goat anti-mouse Alexa Fluor 594 (red) antibody (Invitrogen A11032). Nuclei were stained with DAPI (Sigma 32670). White scale bars represent 10 μm.

Web Resources

The URLs for data presented herein are as follows:

1000 Genomes, http://www.1000genomes.org/
ExAC Browser, http://exac.broadinstitute.org/
dbSNP, http://www.ncbi.nlm.nih.gov/projects/SNP/
Ensembl Genome Browser, http://www.ensembl.org/index.html
NCBI Conserved Domains, http://www.ncbi.nlm.nih.gov/Structure/cdd/wrpsb.cgi
NHLBI Exome Sequencing Project (ESP) Exome Variant Server, http://evs.gs.washington.edu/EVS/
OMIM, http://www.omim.org
Primer3, http://bioinfo.ut.ee/primer3-0.4.0/
RefSeq, http://www.ncbi.nlm.nih.gov/RefSeq
SNP Check, https://secure.ngrl.org.uk/SNPCheck/snpcheck.htm
UniProt, http://www.uniprot.org/uniprot/

References

1. Afzelius, B.A. (1976). A human syndrome caused by immotile cilia. Science *193*, 317–319.
2. Afzelius, B.A. (1985). The immotile-cilia syndrome: a microtubule-associated defect. CRC Crit. Rev. Biochem. *19*, 63–87.
3. Pazour, G.J., Agrin, N., Leszyk, J., and Witman, G.B. (2005). Proteomic analysis of a eukaryotic cilium. J. Cell Biol. *170*, 103–113.
4. Nonaka, S., Yoshiba, S., Watanabe, D., Ikeuchi, S., Goto, T., Marshall, W.F., and Hamada, H. (2005). De novo formation of left-right asymmetry by posterior tilt of nodal cilia. PLoS Biol. *3*, e268.
5. Satir, P., and Christensen, S.T. (2007). Overview of structure and function of mammalian cilia. Annu. Rev. Physiol. *69*, 377–400.
6. Curry, A.M., and Rosenbaum, J.L. (1993). Flagellar radial spoke: a model molecular genetic system for studying organelle assembly. Cell Motil. Cytoskeleton *24*, 224–232.
7. Warner, F.D., and Satir, P. (1974). The structural basis of ciliary bend formation. Radial spoke positional changes accompanying microtubule sliding. J. Cell Biol. *63*, 35–63.
8. Smith, E.F., and Yang, P. (2004). The radial spokes and central apparatus: mechano-chemical transducers that regulate flagellar motility. Cell Motil. Cytoskeleton *57*, 8–17.
9. Oda, T., Yanagisawa, H., Yagi, T., and Kikkawa, M. (2014). Mechanosignaling between central apparatus and radial spokes controls axonemal dynein activity. J. Cell Biol. *204*, 807–819.
10. Lin, J., Yin, W., Smith, M.C., Song, K., Leigh, M.W., Zariwala, M.A., Knowles, M.R., Ostrowski, L.E., and Nicastro, D. (2014). Cryo-electron tomography reveals ciliary defects underlying human RSPH1 primary ciliary dyskinesia. Nat. Commun. *5*, 5727.
11. Pennarun, G., Escudier, E., Chapelin, C., Bridoux, A.M., Cacheux, V., Roger, G., Clément, A., Goossens, M., Amselem, S., and Duriez, B. (1999). Loss-of-function mutations in a human gene related to Chlamydomonas reinhardtii dynein IC78 result in primary ciliary dyskinesia. Am. J. Hum. Genet. *65*, 1508–1519.
12. Loges, N.T., Olbrich, H., Fenske, L., Mussaffi, H., Horvath, J., Fliegauf, M., Kuhl, H., Baktai, G., Peterffy, E., Chodhari, R., et al. (2008). DNAI2 mutations cause primary ciliary dyskinesia with defects in the outer dynein arm. Am. J. Hum. Genet. *83*, 547–558.
13. Olbrich, H., Häffner, K., Kispert, A., Völkel, A., Volz, A., Sasmaz, G., Reinhardt, R., Hennig, S., Lehrach, H., Konietzko, N., et al. (2002). Mutations in DNAH5 cause primary ciliary dyskinesia and randomization of left-right asymmetry. Nat. Genet. *30*, 143–144.
14. Duriez, B., Duquesnoy, P., Escudier, E., Bridoux, A.-M., Escalier, D., Rayet, I., Marcos, E., Vojtek, A.-M., Bercher, J.-F., and Amselem, S. (2007). A common variant in combination with a nonsense mutation in a member of the thioredoxin family causes primary ciliary dyskinesia. Proc. Natl. Acad. Sci. USA *104*, 3336–3341.
15. Mazor, M., Alkrinawi, S., Chalifa-Caspi, V., Manor, E., Sheffield, V.C., Aviram, M., and Parvari, R. (2011). Primary ciliary dyskinesia caused by homozygous mutation in DNAL1, encoding dynein light chain 1. Am. J. Hum. Genet. *88*, 599–607.
16. Onoufriadis, A., Paff, T., Antony, D., Shoemark, A., Micha, D., Kuyt, B., Schmidts, M., Petridi, S., Dankert-Roelse, J.E., Haarman, E.G., et al.; UK10K (2013). Splice-site mutations in the axonemal outer dynein arm docking complex gene CCDC114 cause primary ciliary dyskinesia. Am. J. Hum. Genet. *92*, 88–98.
17. Knowles, M.R., Leigh, M.W., Ostrowski, L.E., Huang, L., Carson, J.L., Hazucha, M.J., Yin, W., Berg, J.S., Davis, S.D., Dell, S.D., et al.; Genetic Disorders of Mucociliary Clearance Consortium (2013). Exome sequencing identifies mutations in CCDC114 as a cause of primary ciliary dyskinesia. Am. J. Hum. Genet. *92*, 99–106.
18. Duquesnoy, P., Escudier, E., Vincensini, L., Freshour, J., Bridoux, A.-M., Coste, A., Deschildre, A., de Blic, J., Legendre, M., Montantin, G., et al. (2009). Loss-of-function mutations in the human ortholog of Chlamydomonas reinhardtii ODA7 disrupt dynein arm assembly and cause primary ciliary dyskinesia. Am. J. Hum. Genet. *85*, 890–896.
19. Loges, N.T., Olbrich, H., Becker-Heck, A., Häffner, K., Heer, A., Reinhard, C., Schmidts, M., Kispert, A., Zariwala, M.A., Leigh, M.W., et al. (2009). Deletions and point mutations of LRRC50 cause primary ciliary dyskinesia due to dynein arm defects. Am. J. Hum. Genet. *85*, 883–889.
20. Omran, H., Kobayashi, D., Olbrich, H., Tsukahara, T., Loges, N.T., Hagiwara, H., Zhang, Q., Leblond, G., O'Toole, E., Hara, C., et al. (2008). Ktu/PF13 is required for cytoplasmic pre-assembly of axonemal dyneins. Nature *456*, 611–616.
21. Mitchison, H.M., Schmidts, M., Loges, N.T., Freshour, J., Dritsoula, A., Hirst, R.A., O'Callaghan, C., Blau, H., Al Dabbagh, M., Olbrich, H., et al. (2012). Mutations in axonemal dynein assembly factor DNAAF3 cause primary ciliary dyskinesia. Nat. Genet. *44*, 381–389, S1–S2.
22. Kott, E., Duquesnoy, P., Copin, B., Legendre, M., Dastot-Le Moal, F., Montantin, G., Jeanson, L., Tamalet, A., Papon, J.-F., Siffroi, J.-P., et al. (2012). Loss-of-function mutations in LRRC6, a gene essential for proper axonemal assembly of inner and outer dynein arms, cause primary ciliary dyskinesia. Am. J. Hum. Genet. *91*, 958–964.
23. Horani, A., Druley, T.E., Zariwala, M.A., Patel, A.C., Levinson, B.T., Van Arendonk, L.G., Thornton, K.C., Giacalone, J.C., Albee, A.J., Wilson, K.S., et al. (2012). Whole-exome capture and sequencing identifies HEATR2 mutation as a cause of primary ciliary dyskinesia. Am. J. Hum. Genet. *91*, 685–693.
24. Panizzi, J.R., Becker-Heck, A., Castleman, V.H., Al-Mutairi, D.A., Liu, Y., Loges, N.T., Pathak, N., Austin-Tse, C., Sheridan, E., Schmidts, M., et al. (2012). CCDC103 mutations cause primary ciliary dyskinesia by disrupting assembly of ciliary dynein arms. Nat. Genet. *44*, 714–719.

25. Merveille, A.-C., Davis, E.E., Becker-Heck, A., Legendre, M., Amirav, I., Bataille, G., Belmont, J., Beydon, N., Billen, F., Clément, A., et al. (2011). CCDC39 is required for assembly of inner dynein arms and the dynein regulatory complex and for normal ciliary motility in humans and dogs. Nat. Genet. *43*, 72–78.
26. Becker-Heck, A., Zohn, I.E., Okabe, N., Pollock, A., Lenhart, K.B., Sullivan-Brown, J., McSheene, J., Loges, N.T., Olbrich, H., Haeffner, K., et al. (2011). The coiled-coil domain containing protein CCDC40 is essential for motile cilia function and left-right axis formation. Nat. Genet. *43*, 79–84.
27. Hjeij, R., Lindstrand, A., Francis, R., Zariwala, M.A., Liu, X., Li, Y., Damerla, R., Dougherty, G.W., Abouhamed, M., Olbrich, H., et al. (2013). ARMC4 mutations cause primary ciliary dyskinesia with randomization of left/right body asymmetry. Am. J. Hum. Genet. *93*, 357–367.
28. Hjeij, R., Onoufriadis, A., Watson, C.M., Slagle, C.E., Klena, N.T., Dougherty, G.W., Kurkowiak, M., Loges, N.T., Diggle, C.P., Morante, N.F.C., et al.; UK10K Consortium (2014). CCDC151 mutations cause primary ciliary dyskinesia by disruption of the outer dynein arm docking complex formation. Am. J. Hum. Genet. *95*, 257–274.
29. Knowles, M.R., Ostrowski, L.E., Loges, N.T., Hurd, T., Leigh, M.W., Huang, L., Wolf, W.E., Carson, J.L., Hazucha, M.J., Yin, W., et al. (2013). Mutations in SPAG1 cause primary ciliary dyskinesia associated with defective outer and inner dynein arms. Am. J. Hum. Genet. *93*, 711–720.
30. Tarkar, A., Loges, N.T., Slagle, C.E., Francis, R., Dougherty, G.W., Tamayo, J.V., Shook, B., Cantino, M., Schwartz, D., Jahnke, C., et al.; UK10K (2013). DYX1C1 is required for axonemal dynein assembly and ciliary motility. Nat. Genet. *45*, 995–1003.
31. Zariwala, M.A., Gee, H.Y., Kurkowiak, M., Al-Mutairi, D.A., Leigh, M.W., Hurd, T.W., Hjeij, R., Dell, S.D., Chaki, M., Dougherty, G.W., et al. (2013). ZMYND10 is mutated in primary ciliary dyskinesia and interacts with LRRC6. Am. J. Hum. Genet. *93*, 336–345.
32. Austin-Tse, C., Halbritter, J., Zariwala, M.A., Gilberti, R.M., Gee, H.Y., Hellman, N., Pathak, N., Liu, Y., Panizzi, J.R., Patel-King, R.S., et al. (2013). Zebrafish Ciliopathy Screen Plus Human Mutational Analysis Identifies C21orf59 and CCDC65 Defects as Causing Primary Ciliary Dyskinesia. Am. J. Hum. Genet. *93*, 672–686.
33. Moore, A., Escudier, E., Roger, G., Tamalet, A., Pelosse, B., Marlin, S., Clément, A., Geremek, M., Delaisi, B., Bridoux, A.-M., et al. (2006). RPGR is mutated in patients with a complex X linked phenotype combining primary ciliary dyskinesia and retinitis pigmentosa. J. Med. Genet. *43*, 326–333.
34. Bartoloni, L., Blouin, J.-L., Pan, Y., Gehrig, C., Maiti, A.K., Scamuffa, N., Rossier, C., Jorissen, M., Armengot, M., Meeks, M., et al. (2002). Mutations in the DNAH11 (axonemal heavy chain dynein type 11) gene cause one form of situs inversus totalis and most likely primary ciliary dyskinesia. Proc. Natl. Acad. Sci. USA *99*, 10282–10286.
35. Wirschell, M., Olbrich, H., Werner, C., Tritschler, D., Bower, R., Sale, W.S., Loges, N.T., Pennekamp, P., Lindberg, S., Stenram, U., et al. (2013). The nexin-dynein regulatory complex subunit DRC1 is essential for motile cilia function in algae and humans. Nat. Genet. *45*, 262–268.
36. Horani, A., Brody, S.L., Ferkol, T.W., Shoseyov, D., Wasserman, M.G., Ta-shma, A., Wilson, K.S., Bayly, P.V., Amirav, I., Cohen-Cymberknoh, M., et al. (2013). CCDC65 mutation causes primary ciliary dyskinesia with normal ultrastructure and hyperkinetic cilia. PLoS ONE *8*, e72299.
37. Nakhleh, N., Francis, R., Giese, R.A., Tian, X., Li, Y., Zariwala, M.A., Yagi, H., Khalifa, O., Kureshi, S., Chatterjee, B., et al. (2012). High prevalence of respiratory ciliary dysfunction in congenital heart disease patients with heterotaxy. Circulation *125*, 2232–2242.
38. Castleman, V.H., Romio, L., Chodhari, R., Hirst, R.A., de Castro, S.C.P., Parker, K.A., Ybot-Gonzalez, P., Emes, R.D., Wilson, S.W., Wallis, C., et al. (2009). Mutations in radial spoke head protein genes RSPH9 and RSPH4A cause primary ciliary dyskinesia with central-microtubular-pair abnormalities. Am. J. Hum. Genet. *84*, 197–209.
39. Ziętkiewicz, E., Bukowy-Bieryłło, Z., Voelkel, K., Klimek, B., Dmeńska, H., Pogorzelski, A., Sulikowska-Rowińska, A., Rutkiewicz, E., and Witt, M. (2012). Mutations in radial spoke head genes and ultrastructural cilia defects in East-European cohort of primary ciliary dyskinesia patients. PLoS ONE *7*, e33667.
40. Alsaadi, M.M., Gaunt, T.R., Boustred, C.R., Guthrie, P.A.I., Liu, X., Lenzi, L., Rainbow, L., Hall, N., Alharbi, K.K., and Day, I.N.M. (2012). From a single whole exome read to notions of clinical screening: primary ciliary dyskinesia and RSPH9 p.Lys268del in the Arabian Peninsula. Ann. Hum. Genet. *76*, 211–220.
41. Kott, E., Legendre, M., Copin, B., Papon, J.-F., Dastot-Le Moal, F., Montantin, G., Duquesnoy, P., Piterboth, W., Amram, D., Bassinet, L., et al. (2013). Loss-of-function mutations in RSPH1 cause primary ciliary dyskinesia with central-complex and radial-spoke defects. Am. J. Hum. Genet. *93*, 561–570.
42. Olbrich, H., Schmidts, M., Werner, C., Onoufriadis, A., Loges, N.T., Raidt, J., Banki, N.F., Shoemark, A., Burgoyne, T., Al Turki, S., et al.; UK10K Consortium (2012). Recessive HYDIN mutations cause primary ciliary dyskinesia without randomization of left-right body asymmetry. Am. J. Hum. Genet. *91*, 672–684.
43. Vallet, C., Escudier, E., Roudot-Thoraval, F., Blanchon, S., Fauroux, B., Beydon, N., Boulé, M., Vojtek, A.M., Amselem, S., Clément, A., and Tamalet, A. (2013). Primary ciliary dyskinesia presentation in 60 children according to ciliary ultrastructure. Eur. J. Pediatr. *172*, 1053–1060.
44. Papon, J.F., Coste, A., Roudot-Thoraval, F., Boucherat, M., Roger, G., Tamalet, A., Vojtek, A.M., Amselem, S., and Escudier, E. (2010). A 20-year experience of electron microscopy in the diagnosis of primary ciliary dyskinesia. Eur. Respir. J. *35*, 1057–1063.
45. Tamalet, A., Clement, A., Roudot-Thoraval, F., Desmarquest, P., Roger, G., Boulé, M., Millepied, M.C., Baculard, T.A., and Escudier, E. (2001). Abnormal central complex is a marker of severity in the presence of partial ciliary defect. Pediatrics *108*, E86.
46. Rossman, C.M., Lee, R.M., Forrest, J.B., and Newhouse, M.T. (1984). Nasal ciliary ultrastructure and function in patients with primary ciliary dyskinesia compared with that in normal subjects and in subjects with various respiratory diseases. Am. Rev. Respir. Dis. *129*, 161–167.
47. Jivan, A., Earnest, S., Juang, Y.-C., and Cobb, M.H. (2009). Radial spoke protein 3 is a mammalian protein kinase A-anchoring protein that binds ERK1/2. J. Biol. Chem. *284*, 29437–29445.
48. Diener, D.R., Ang, L.H., and Rosenbaum, J.L. (1993). Assembly of flagellar radial spoke proteins in Chlamydomonas:

identification of the axoneme binding domain of radial spoke protein 3. J. Cell Biol. *123*, 183–190.
49. Yang, C., and Yang, P. (2006). The flagellar motility of Chlamydomonas pf25 mutant lacking an AKAP-binding protein is overtly sensitive to medium conditions. Mol. Biol. Cell *17*, 227–238.
50. Sivadas, P., Dienes, J.M., St Maurice, M., Meek, W.D., and Yang, P. (2012). A flagellar A-kinase anchoring protein with two amphipathic helices forms a structural scaffold in the radial spoke complex. J. Cell Biol. *199*, 639–651.
51. Gupta, A., Diener, D.R., Sivadas, P., Rosenbaum, J.L., and Yang, P. (2012). The versatile molecular complex component LC8 promotes several distinct steps of flagellar assembly. J. Cell Biol. *198*, 115–126.
52. Breathnach, R., Benoist, C., O'Hare, K., Gannon, F., and Chambon, P. (1978). Ovalbumin gene: evidence for a leader sequence in mRNA and DNA sequences at the exon-intron boundaries. Proc. Natl. Acad. Sci. USA *75*, 4853–4857.
53. Papon, J.-F., Bassinet, L., Cariou-Patron, G., Zerah-Lancner, F., Vojtek, A.-M., Blanchon, S., Crestani, B., Amselem, S., Coste, A., Housset, B., et al. (2012). Quantitative analysis of ciliary beating in primary ciliary dyskinesia: a pilot study. Orphanet J. Rare Dis. *7*, 78.
54. Frommer, A., Hjeij, R., Loges, N.T., Edelbusch, C., Jahnke, C., Raidt, J., Werner, C., Wallmeier, J., Große-Onnebrink, J., Olbrich, H., et al. (2015). Immunofluorescence Analysis and Diagnosis of Primary Ciliary Dyskinesia with Radial Spoke Defects. Am. J. Respir. Cell Mol. Biol. Published online on March 19, 2015.
55. Mitchell, D.R., and Sale, W.S. (1999). Characterization of a Chlamydomonas insertional mutant that disrupts flagellar central pair microtubule-associated structures. J. Cell Biol. *144*, 293–304.
56. Huang, B., Piperno, G., Ramanis, Z., and Luck, D.J. (1981). Radial spokes of Chlamydomonas flagella: genetic analysis of assembly and function. J. Cell Biol. *88*, 80–88.
57. Diener, D.R., Yang, P., Geimer, S., Cole, D.G., Sale, W.S., and Rosenbaum, J.L. (2011). Sequential assembly of flagellar radial spokes. Cytoskeleton (Hoboken) *68*, 389–400.
58. Hirokawa, N., Tanaka, Y., and Okada, Y. (2009). Left-right determination: involvement of molecular motor KIF3, cilia, and nodal flow. Cold Spring Harb. Perspect. Biol. *1*, a000802.
59. Stannard, W., Rutman, A., Wallis, C., and O'Callaghan, C. (2004). Central microtubular agenesis causing primary ciliary dyskinesia. Am. J. Respir. Crit. Care Med. *169*, 634–637.